Inorganic Chemistry

Article

pubs.acs.org/IC

2-Aminoisobutyric Acid in Co(II) and Co(II)/Ln(III) Chemistry: Homometallic and Heterometallic Clusters

George J. Sopasis,[†,‡] Maria Orfanoudaki,[†] Pavlos Zarmpas,[†] Aggelos Philippidis,[§] Milosz Siczek,[∥] Tadeusz Lis,[∥] James R. O'Brien,[⊥] and Constantinos J. Milios*,[†]

[†]Department of Chemistry, The University of Crete, Voutes 71003, Herakleion, Greece

[‡]Department of Materials Science and Technology, The University of Crete, Voutes 71003, Herakleion, Greece

[§]Institute of Electronic Structure and Laser, Foundation for Research and Technology—Hellas (IESL-FORTH), P.O. Box 1385, GR 711 10 Herakleion, Crete, Greece

[∥]Faculty of Chemistry, The University of Wroclaw, Joliot-Curie 14, 50-383 Wroclaw, Poland

[⊥]Quantum Design, San Diego, California 92121, United States

Ⓢ *Supporting Information*

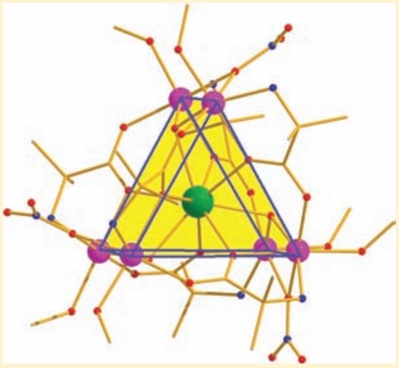

ABSTRACT: The synthesis and magnetic properties of 13 new homo- and heterometallic Co(II) complexes containing the artificial amino acid 2-amino-isobutyric acid, aibH, are reported: $[Co^{II}_4(aib)_3(aibH)_3(NO_3)](NO_3)_4\cdot 2.8CH_3OH\cdot 0.2H_2O$ ($\mathbf{1}\cdot 2.8CH_3OH\cdot 0.2H_2O$), $\{Na_2[Co^{II}_2(aib)_2(N_3)_4(CH_3OH)_4]\}_n$ (**2**), $[Co^{II}_6La^{III}(aib)_6(OH)_3(NO_3)_2(H_2O)_4(CH_3CN)_2]\cdot 0.5[La(NO_3)_6]\cdot 0.75(ClO_4)\cdot 1.75(NO_3)\cdot 3.2CH_3CN\cdot 5.9H_2O$ ($\mathbf{3}\cdot 3.2CH_3CN\cdot 5.9H_2O$), $[Co^{II}_6Pr^{III}(aib)_6(OH)_3(NO_3)_3(CH_3CN)_6]\cdot[Pr(NO_3)_5]\cdot 0.41[Pr(NO_3)_3(ClO_4)_{0.5}(H_2O)_{1.5}]\cdot 0.59[Co(NO_3)_3(H_2O)]\cdot 0.2(ClO_4)\cdot 0.25H_2O$ ($\mathbf{4}\cdot 0.25H_2O$), $[Co^{II}_6Nd^{III}(aib)_6(OH)_3(NO_3)_{2.8}(CH_3OH)_{4.7}(H_2O)_{1.5}]\cdot 2.7(ClO_4)\cdot 0.5(NO_3)\cdot 2.26CH_3OH\cdot 0.24H_2O$ ($\mathbf{5}\cdot 2.26CH_3OH\cdot 0.24H_2O$), $[Co^{II}_6Sm^{III}(aib)_6(OH)_3(NO_3)_3(CH_3CN)_6]\cdot[Sm(NO_3)_5]\cdot 0.44[Sm(NO_3)_3(ClO_4)_{0.5}(H_2O)_{1.5}]\cdot 0.56[Co(NO_3)_3(H_2O)]\cdot 0.22(ClO_4)\cdot 0.3H_2O$ ($\mathbf{6}\cdot 0.3H_2O$), $[Co^{II}_6Eu^{III}(aib)_6(OH)_3(NO_3)_3(CH_3OH)_{4.87}(H_2O)_{1.13}](ClO_4)_{2.5}(NO_3)_{0.5}\cdot 2.43CH_3OH\cdot 0.92H_2O$ ($\mathbf{7}\cdot 2.43CH_3OH\cdot 0.92H_2O$), $[Co^{II}_6Gd^{III}(aib)_6(OH)_3(NO_3)_{2.9}(CH_3OH)_{4.9}(H_2O)_{1.2}]\cdot 2.6(ClO_4)\cdot 0.5(NO_3)\cdot 2.58CH_3OH\cdot 0.47H_2O$ ($\mathbf{8}\cdot 2.58CH_3OH\cdot 0.47H_2O$), $[Co^{II}_6Tb^{III}(aib)_6(OH)_3(NO_3)_3(CH_3CN)_6]\cdot[Tb(NO_3)_5]\cdot 0.034[Tb(NO_3)_3(ClO_4)_{0.5}(H_2O)_{0.5}]\cdot 0.656[Co(NO_3)_3(H_2O)]\cdot 0.343(ClO_4)\cdot 0.3H_2O$ ($\mathbf{9}\cdot 0.3H_2O$), $[Co^{II}_6Dy^{III}(aib)_6(OH)_3(NO_3)_{2.9}(CH_3OH)_{4.92}(H_2O)_{1.18}](ClO_4)_{2.6}(NO_3)_{0.5}\cdot 2.5CH_3OH\cdot 0.5H_2O$ ($\mathbf{10}\cdot 2.5CH_3OH\cdot 0.5H_2O$), $[Co^{II}_6Ho^{III}(aib)_6(OH)_3(NO_3)_3(CH_3CN)_6]\cdot 0.27[Ho(NO_3)_3(ClO_4)_{0.35}(H_2O)_{0.15}]\cdot 0.656[Co(NO_3)_3(H_2O)]\cdot 0.171(ClO_4)$ (**11**), $[Co^{II}_6Er^{III}(aib)_6(OH)_4(NO_3)_2(CH_3CN)_{2.5}(H_2O)_{3.5}](ClO_4)_3\cdot CH_3CN\cdot 0.75H_2O$ ($\mathbf{12}\cdot CH_3CN\cdot 0.75H_2O$), and $[Co^{II}_6Tm^{III}(aib)_6(OH)_3(NO_3)_3(H_2O)_6]\cdot 1.48(ClO_4)\cdot 1.52(NO_3)\cdot 3H_2O$ ($\mathbf{13}\cdot 3H_2O$). Complex **1** describes a distorted tetrahedral metallic cluster, while complex **2** can be considered to be a 2-D coordination polymer. Complexes **3**−**13** can all be regarded as metallo-cryptand encapsulated lanthanides in which the central lanthanide ion is captivated within a $[Co^{II}_6]$ trigonal prism. dc and ac magnetic susceptibility studies have been carried out in the 2−300 K range for complexes **1**, **3**, **5**, **7**, **8**, **10**, **12**, and **13**, revealing the possibility of single molecule magnetism behavior for complex **10**.

INTRODUCTION

The synthesis of polynuclear cluster compounds has increased greatly in recent years due to the potential that such compounds display for new technological applications.[1] In the field of *molecule-based magnetism*, that deals with the study of the magnetic properties of discrete molecular species and/or polymeric materials, a major breakthrough was the discovery that molecular complexes can function as nanodimensional magnets at very low temperatures in the absence of an external magnetic field, retaining their magnetization once magnetized.[2] This phenomenon, termed single molecule magnetism (SMM) and initially involving 3d metals such as Mn and Fe, has now been expanded to include other 3d- and 4f-block metal ions as well.[3] The lanthanides entered the SMM field recently, *albeit* with great potential, and this is also true for both heterometallic 3d−4f, and homometallic 4f clusters.[4] The reasons why lanthanides are now considered as major candidates in the SMM field are dual: (i) their large magnetic moments and (ii) their spin−orbit coupling based magnetic anisotropy (with the exceptions of La^{III}, Gd^{III}, and Lu^{III}). Both provide a good starting point for the synthesis of SMMs. In addition, lanthanide-based clusters can display fascinating photoluminescent properties, and as such, they are candidates for applications in areas such as light emitting diodes, optical fibers, lasers, optical amplifiers, NIR-emitting materials, and sensory

Received: November 7, 2011
Published: December 22, 2011

dx.doi.org/10.1021/ic2024007 | *Inorg. Chem.* 2012, 51, 1170−1179

probes.[5] This is mainly due to the electronic properties of the lanthanide ions: the shielding of the 4f electrons by the outer 5s and 5p electrons results in well-defined absorption and emission bands. As a consequence, the lanthanides retain their atomic properties upon complex formation. Characteristic examples of luminescent lanthanides are Eu^{3+}, Tb^{3+}, and Dy^{3+} complexes which luminesce with red, green, and yellow-orange colors due to $^5D_0 \rightarrow {}^7F_6$, $^5D_4 \rightarrow {}^7F_0$, and $^4F_{9/2} \rightarrow {}^6F_{3/2}$ transitions, respectively.[6] Furthermore, Tm^{3+} is a blue emitter and is being used in electroluminescent devices,[7] while Nd^{3+}, Ho^{3+}, Er^{3+}, and Yb^{3+} emit in the NIR range and, therefore, find applications in laser science and technology.[8]

With the above in mind, we recently initiated a project to examine the Co^{2+}/Ln^{3+}/aibH synthetic system, where aibH is 2-aminoisobutyric acid (Scheme 1), as a means of preparing polymetallic clusters that may display interesting physical properties. This is the first time that the aibH ligand has been employed in polynuclear Co^{II} and/or Co^{II}/Ln chemistry, following on from our initial studies of Ni^{2+} and Ni^{2+}/Ln^{3+} chemistry.[9] Herein we report the syntheses, structures, and magnetic properties of 14 new homo- and heterometallic clusters built with this artificial amino acid. A small part of this work has been previously communicated.[10]

Scheme 1. Structure of 2-Aminoisobutyric Acid, aibH, and Its Coordination Modes in 1−14

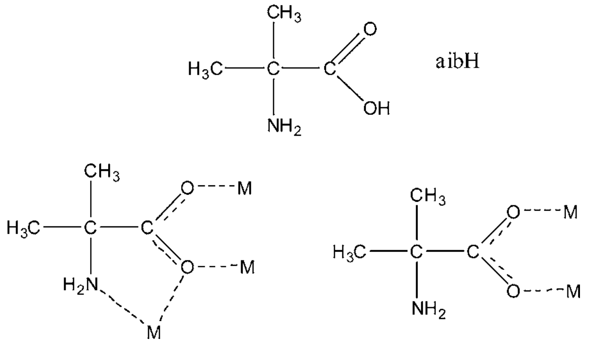

■ EXPERIMENTAL SECTION

All manipulations were performed under aerobic conditions, using materials as received. ***Caution!*** *Although no problems were encountered in this work, care should be taken when using the potentially explosive perchlorate and azide anions.*

$[Co_4(aib)_3(aibH)_3(NO_3)](NO_3)_4 \cdot 2.8MeOH \cdot 0.2H_2O$ ($1 \cdot 2.8MeOH \cdot 0.2H_2O$). To a stirred solution of $Co(NO_3)_2 \cdot 6H_2O$ (291 mg, 1 mmol) in MeOH (30 mL) was added aibH (103 mg, 1 mmol) and NMe_4OH (2 mmol). The resulting pink solution was left stirring for 30 min, during which time it did not change color. The solution was then filtered and layered with Et_2O (20 mL). Pale pink crystals of $[Co_4(aib)_3(aibH)_3(NO_3)](NO_3)_4 \cdot 2.8MeOH \cdot 0.2H_2O$ ($1 \cdot 2.8MeOH \cdot 0.2H_2O$) formed during 4 days in ~30% yield. Anal. Calcd (Found) for $[Co_4(aib)_3(aibH)_3(NO_3)](NO_3)_4$ (**1**): C, 24.82 (24.94); H, 4.43 (4.28); N, 13.27 (13.11)%.

$\{Na_2[Co^{II}_2(aib)_2(N_3)_4(MeOH)_4(H_2O)_2]\}_n$ (2). To a stirred solution of $Co(NO_3)_2 \cdot 6H_2O$ (291 mg, 1 mmol) and aibH (103 mg, 1 mmol) in MeOH (30 mL) was added NaN_3 (195 mg, 3 mmol) and NMe_4OH (2 mmol). The resulting pale pink solution was left stirring for 2 h, during which time the solution darkened to pink. The solution was then filtered and layered with Et_2O (20 mL) to form pink crystals of $\{Na_2[Co^{II}_2(aib)_2(N_3)_4(MeOH)_4(H_2O)_2]\}_n$ (**2**) after 3 days in ~25% yield. Anal. Calcd (Found) for $\{Na_2[Co^{II}_2(aib)_2(N_3)_4(MeOH)_4(H_2O)_2]\}_n$ (**2**): C, 20.58 (20.46); H, 5.19 (4.97); N, 28.00 (28.11)%.

General Synthetic Strategy Applicable to 3−13. To pale pink solutions of $Co(ClO_4)_2 \cdot 6H_2O$ and the corresponding $Ln(NO_3)_3 \cdot 6H_2O$ in MeOH (EtOH or MeCN) were added equivalent amounts of aibH and NMe_4OH (or NEt_3). The solutions were left stirring for ~50 min, filtered, and then layered with Et_2O. In each case, suitable single crystals for X-ray crystallography grew after a period of 3−6 days in 25−45% yields. Elem Anal. Calcd (Found) for dried **3** solvent free: C, 17.86 (17.69); H, 3.16 (3.01); N, 10.97 (11.11). **4**: C, 21.65 (21.52); H, 3.58 (3.39); N, 16.14 (16.01). **5**: C, 18.97 (19.19); H, 4.05 (3.49); N, 7.19 (6.93). **6**: C, 27.07 (26.94); H, 4.53 (4.34); N, 20.18 (20.29). **7**: C, 19.21 (19.34); H, 4.06 (3.92); N, 7.34 (7.25). **8**: C, 19.38 (19.09); H, 4.09 (3.91); N, 7.01 (7.19). **9**: C, 17.91 (17.87); H, 2.95 (2.77); N, 13.35 (13.44). **10**: C, 19.11 (19.22); H, 3.98 (3.89); N, 7.30 (7.22). **11**: C, 21.16 (21.03); H, 3.52 (3.39); N, 15.77 (15.89). **12**: C, 19.52 (19.64); H, 3.47 (3.77); N, 8.24 (8.39). **13**: C, 16.74 (16.67); H, 3.69 (3.41); N, 8.54 (8.69).

Physical Methods. Elemental analyses (C, H, N) were performed by the University of Ioannina microanalysis service. Variable-temperature, solid-state direct current (dc), magnetic susceptibility data down to 2.0 K were collected on a Quantum Design MPMS-XL SQUID magnetometer equipped with a 5 T dc magnet at the University of Crete. Diamagnetic corrections were applied to the observed paramagnetic susceptibilities using Pascal's constants.

X-ray Crystallography and Structure Solution. Data collection parameters and structure solution and refinement details are listed in Tables 1 and 2. Full details for **1**−**6**, **8**−**9**, and **11**−**13** can be found in the CIF files provided in the Supporting Information. Full details for **7** and **10** can be found in the CIF files with CCDC numbers 807048 and 807049, respectively.

■ RESULTS AND DISCUSSION

Synthesis. The reaction between $Co(NO_3)_2 \cdot 6H_2O$ and aibH in the presence of base (NMe_4OH) in MeOH gives the complex $[Co_4(aib)_3(aibH)_3(NO_3)](NO_3)_4$ (**1**), which was crystallographically identified as $1 \cdot 2.8MeOH \cdot 0.2H_2O$. Changing the Co^{II} salt to $Co(ClO_4)_2 \cdot 6H_2O$ did not yield any crystalline material, probably indicating the preference of **1** for nitrate ions given the presence of the bonded monodentate nitrate (*vide infra*). Furthermore, employment of NEt_3 instead of NMe_4OH in the reaction led to the same product as identified by IR spectroscopy. With the identity of complex **1** established, the next step was to investigate whether the presence of additional bridging ligands would affect the identity of complex **1**. Therefore, we repeated the same procedure in the presence of azide ligands, since it is widely known that the N_3^- ligands can increase the nuclearity of a complex by bridging additional metal centers and can also propagate ferromagnetic interactions when in the *end-on* bridging mode.[11] Indeed, employment of the azide ligand led to the formation of $\{Na_2[Co^{II}_2(aib)_2(N_3)_4(MeOH)_4(H_2O)_2]\}_n$ (**2**), which can be considered as a 2-D coordination polymer based on magnetically isolated monomeric $[Co(aib)_2(N_3)_2]^{2-}$ units.

The next step for us was to investigate whether heterometallic Co/Ln species could be isolated by the use of the aibH ligand, especially since we recently started investigating (i) the employment of the aibH ligand in Ni^{2+} and Ni^{2+}/Ln^{3+} chemistry[9] and (ii) the similarity between Ni^{2+} and Co^{2+} cluster chemistry. Therefore, following the procedure used for the synthesis of Ni^{2+}/Ln^{3+} clusters, we started by using the diamagnetic La^{3+} and continued across the whole lanthanide period (omitting the radioactive Pm^{3+} and the diamagnetic Lu^{3+}). The synthesis of the clusters was straightforward: reaction of a Co^{II} salt $[Co(ClO_4)_2 \cdot 6H_2O]$ with the corresponding $Ln(NO_3)_3 \cdot 6H_2O$ and aibH in alcohol (ROH, R = Me, Et) or MeCN in the presence of a base (NMe_4OH, NEt_4OH, NH_4OH, or NEt_3) afforded the heterometallic complexes containing the metallic

Table 1. Crystallographic Data for Complexes 1−5

	1·2.8CH$_3$OH· 0.2H$_2$O	**2**	**3**·3.2CH$_3$CN·5.9H$_2$O	**4**·0.25H$_2$O	**5**
formula[a]	$C_{31.80}H_{82.60}Co_4N_{11}O_{35}$	$C_{10}H_{24}CoN_8NaO_6$	$C_{31.2}H_{76.08}Cl_{0.75}Co_6La_{1.5}N_{16.35}O_{45.15}$	$C_{36}H_{71.91}Cl_{0.416}Co_{6.584}N_{23}O_{51.12}Pr_{2.416}$	$C_{30.917}H_{83.21}Cl_{2.70}Co_6N_{9.30}NdO_{44.94}$
M_W	1415.01	434.29	1991.40	2388.08	1898.04
crystal system	triclinic	monoclinic	monoclinic	hexagonal	triclinic
space group	$P\bar{1}$	$P2_1/c$	$C2/c$	$P6_3/m$	$P\bar{1}$
a/Å	12.019 (5)	12.426 (5)	51.59 (2)	14.972 (4)	13.208 (4)
b/Å	12.521 (5)	15.162 (6)	14.994 (5)		13.742 (4)
c/Å	21.999 (9)	11.390 (5)	21.710 (7)	22.300 (9)	22.143 (8)
α/deg	91.31 (4)				86.80 (4)
β/deg	102.14 (4)	114.88 (4)	109.83 (4)		81.29 (4)
γ/deg	102.33 (4)				62.31 (5)
V/Å^3	3154 (2)	1946.7 (14)	15798 (10)	4329 (2)	3517 (3)
Z	2	4	8	2	2
T/K	100	100	100	100	100
λ/Å	0.71073	0.71073	0.71073	0.71073	0.71073
D_c/(g cm^{-3})	1.490	1.482	1.675	1.832	1.792
μ(Mo Kα)/mm^{-1}	1.13	0.95	2.15	2.68	2.31
meas/indep (R_{int}) refl	35709/17079 (0.035)	27174/8027 (0.040)	70543/18259 (0.081)	15892/4326 (0.027)	38509/18940 (0.077)
obs refl [$I > 2\sigma(I)$]	10688	5374	9200	2806	9255
$wR2$[b,c]	0.133	0.082	0.191	0.100	0.152
$R1$[c,d]	0.048	0.035	0.066	0.032	0.067
goodness of fit on F^2	1.008	1.009	1.017	1.060	1.008
$\Delta\rho_{max,min}$/(e Å^{-3})	0.80, −0.86	0.75, −0.51	1.38, −1.98	0.72, −0.56	2.09, −1.28

[a] Including solvate molecules Mo Kα radiation, graphite monochromator. [b] $wR2 = [\sum w(|F_o^2| - |F_c^2|)^2/\sum w|F_o^2|^2]^{1/2}$. [c] For observed data. [d] $R1 = \sum||F_o| - |F_c||/\sum|F_o|$.

Table 2. Crystallographic Data for Complexes 6, 8, 9, 11, 12, and 13

	6·0.3H$_2$O	**8**·2.58CH$_3$OH·0.47H$_2$O	**9**·0.3H$_2$O	**11**	**12**·CH$_3$CN·0.75H$_2$O	**13**·3H$_2$O
formula[a]	$C_{36}H_{72.04}Cl_{0.44}Co_{6.56}N_{23}O_{51.56}Sm_{2.44}$	$C_{31.50}H_{84.31}Cl_{2.60}Co_6GdN_{9.40}O_{44.7}$	$C_{36}H_{71.35}Cl_{0.35}Co_{6.656}N_{23}O_{50.54}Tb_{2.344}$	$C_{72}H_{143.90}Cl_{0.54}Co_{13.45}Ho_{4.54}N_{46}O_{101.10}$	$C_{31}H_{71}Cl_3Co_6ErN_{11.50}O_{38.25}$	$C_{24}H_{69}Cl_{1.48}Co_6N_{10.52}O_{43.48}Tm$
M_W	2421.28	1913.99	2412.30	4832.36	1844.18	1775.83
crystal system	hexagonal	triclinic	hexagonal	hexagonal	orthorhombic	hexagonal
space group	$P6_3/m$	$P\bar{1}$	$P6_3/m$	$P6_3/m$	$Pbcm$	$P6_3/m$
a/Å	14.920 (6)	13.197 (4)	15.021 (3)	14.844 (4)	15.225 (5)	12.453 (4)
b/Å		13.729 (5)			21.585 (6)	
c/Å	22.250 (9)	22.221 (7)	22.362 (6)	22.236 (8)	23.839 (7)	22.078 (8)
α/deg		86.94 (3)				
β/deg		81.49 (3)				
γ/deg		62.16 (4)				
V/Å^3	4289 (3)	3520 (2)	4370 (2)	4243 (2)	7834 (4)	2965.1 (17)
Z	2	2	2	1	4	2
T/K	100	100	220	100	100	110
λ/Å	0.71073	0.71073	0.71073	0.71073	0.71073	0.71073
D_c/(g cm^{-3})	1.875	1.806	1.833	1.891	1.564	1.989
μ(Mo Kα)/mm^{-1}	3.00	2.51	3.22	3.49	2.49	3.30
meas/indep (R_{int}) refl	13994/3902 (0.049)	32833/18251 (0.029)	38819/3644 (0.051)	24162/4251 (0.036)	97186/11637 (0.064)	22347/2930 (0.114)
obs refl [$I > 2\sigma(I)$]	1895	12060	2453	2625	7523	1588
$wR2$[b,c]	0.101	0.091	0.080	0.091	0.234	0.036
$R1$[c,d]	0.039	0.041	0.031	0.032	0.069	0.034
goodness of fit on F^2	1.000	1.009	1.008	1.060	1.048	0.813
$\Delta\rho_{max,min}$/(e Å^{-3})	1.08, −0.84	1.36, −0.78	0.72, −0.33	1.10, −0.73	2.32, −1.86	1.20, −1.19

[a] Including solvate molecules Mo Kα radiation, graphite monochromator. [b] $wR2 = [\sum w(|F_o^2| - |F_c^2|)^2/\sum w|F_o^2|^2]^{1/2}$. [c] For observed data. [d] $R1 = \sum||F_o| - |F_c||/\sum|F_o|$.

$[\mathrm{Co^{II}}_6\mathrm{Ln^{III}}]$ core (Ln = La (**3**), Pr (**4**), Nd (**5**), Sm (**6**), Eu (**7**), Gd (**8**), Tb (**9**), Dy (**10**), Ho (**11**), Er (**12**), and Tm (**13**)) in moderate to good yields in 3−6 days. From all 13 $\mathrm{Ln^{3+}}$ centers investigated in the $\mathrm{Co^{2+}/Ln^{3+}}$/aibH system, only $\mathrm{Yb^{3+}}$ did not afford single crystals suitable for X-ray analysis. This may perhaps be attributed to the small radius of the $\mathrm{Yb^{3+}}$ ions. We do not report the $[\mathrm{Co_6Ce}]$ analogue, since we encountered problems for the successful completion of its structural refinement. Yet, this analogue can be obtained by very similar reaction pathways. The clusters also appear to be the thermodynamically favored end-products, since in most of the cases, we were able to isolate the same products using a variety of $\mathrm{Co^{II}}$ starting materials, e.g. $\mathrm{Co(NO_3)_2{\cdot}6H_2O}$ and $\mathrm{Co(OAc)_2{\cdot}4H_2O}$, as well as a variety of bases, e.g. $\mathrm{NEt_3}$, $\mathrm{NEt_4OH}$, $\mathrm{NMe_4OH}$, and $\mathrm{NH_4OH}$.

Only two heterometallic heptanuclear $[\mathrm{Co_6Ln}]$ complexes (Ln = La, Pr) have been isolated and reported in the past with the use of the naturally occurring amino acids proline and glycine, but the metal topology of these clusters was different (*vide infra*).[12] An extensive Co/Ln CCDC search revealed the presence of ∼130 examples of discrete heterometallic Co_n^{+x}/$\mathrm{Ln^{III}}$ clusters ($n \geq 1$; $x = 2, 3$). These can be divided into the following categories: $8\mathrm{Co}_n^{+x}/\mathrm{La^{III}}$, $8\mathrm{Co}_n^{+x}/\mathrm{Ce^{III}}$, $7\mathrm{Co}_n^{+x}/\mathrm{Pr^{III}}$, $7\mathrm{Co}_n^{+x}/\mathrm{Nd^{III}}$, $4\mathrm{Co}_n^{+x}/\mathrm{Sm^{III}}$, $3\mathrm{Co}_n^{+x}/\mathrm{Eu^{III}}$, $17\mathrm{Co}_n^{+x}/\mathrm{Gd^{III}}$, $7\mathrm{Co}_n^{+x}/\mathrm{Tb^{III}}$, $5\mathrm{Co}_n^{+x}/\mathrm{Dy^{III}}$, $1\mathrm{Co}_n^{+x}/\mathrm{Ho^{III}}$, $2\mathrm{Co}_n^{+x}/\mathrm{Er^{III}}$, $1\mathrm{Co}_n^{+x}/\mathrm{Tm^{III}}$, $1\mathrm{Co}_n^{+x}/\mathrm{Yb^{III}}$, and $2\mathrm{Co}_n^{+x}/\mathrm{Lu^{III}}$ clusters, with the remaining 57 complexes being organometallic-based.

Until recently, the coordination chemistry of 2-aminoisobutyric acid was not extensively explored. Besides our work on $\mathrm{Ni^{2+}}$ and $\mathrm{Ni^{2+}/Ln^{3+}}$ chemistry,[9] most of the complexes previously isolated were monomers or dimers,[13] with the only exceptions being an aesthetically impressive $[\mathrm{Cu_{24}Gd_6}]$ complex[14] and a $[\mathrm{Zn_3}]$ complex.[15]

Description of Structures. The structure of complex **1** is shown in Figure 1 with selected bond lengths and angles given in Table S1 of the Supporting Information. The central core of **1** describes a $[\mathrm{Co_4(aib)_3(aibH)_3}]^{5+}$ distorted tetrahedron consisting of $\mathrm{Co^{II}}$ ions linked together by three deprotonated $\mathrm{aib^-}$ ligands in a $\eta^2{:}\eta^1{:}\eta^1{:}\mu_3$ fashion and three aibH ligands in their *zwitterionic* form, found in a *syn, syn* $\eta^1{:}\eta^1{:}\mu$ coordination mode. The base of the tetrahedron consists of a near-planar $[\mathrm{Co_3(aibH)_3}]^{6+}$ unit, with the apical $\mathrm{Co^{II}}$ ion located ∼1.50 Å above the base of the tetrahedron. The dimensions of the metallic tetrahedron are in the range ∼3.49−5.49 Å, with the longer distances between basal $\mathrm{Co^{II}}$ ions and the shortest between the apical $\mathrm{Co^{II}}$ and the basal $\mathrm{Co^{II}}$ ions. The coordination spheres for the Co atoms are completed by MeOH molecules and one $\mathrm{NO_3^-}$ anion terminally bonded to Co4. All Co centers are six-coordinate, adopting distorted octahedral geometries.

In the crystal, the molecules form 2-D sheets that stack in an on-set fashion directly upon one another in a head−tail fashion (Figure 1, right). The disordered counterions (nitrates) and the solvate molecules make a detailed analysis of the crystal lattice interactions nontrivial, and thus, we avoid discussing it further.

The structure of complex **2** is shown in Figure 2, with selected bond lengths and angles given in Table S2 of the Supporting Information. The ingredients have been assembled to form a two-dimensional undulated framework parallel to the *bc* plane. In this arrangement, the $[\mathrm{Na_2}]^{2+}$ subunits act as 4-connected nodes with the $[\mathrm{Co(aib)_2(N_3)_2}]^{2-}$ anions bridging them in a bent fashion resulting in a (4,4) network. The $\mathrm{aib^-}$ ligands are found in two coordination modes: $\eta^1{:}\eta^1{:}\eta^1{:}\mu$ bridging one $\mathrm{Co^{II}}$ and one $\mathrm{Na^+}$ ion, and $\eta^2{:}\eta^2{:}\eta^1{:}\mu_3$ bridging one $\mathrm{Co^{II}}$ and two $\mathrm{Na^+}$ ions. The azide ligands are terminally bonded to the $\mathrm{Co^{II}}$ centers. Each Co center is six-coordinate, adopting a slightly distorted octahedral geometry. Given that the $\mathrm{Na^+}$ ions form purely electrostatic and not coordination bonds, the structure may be alternatively described as a $\mathrm{Na_2[Co(aib)_2(N_3)_2]{\cdot}4MeOH}$ monomer.

Complexes **3**−**13** are essentially isostructural (Figure 3), with the differences being the counterions present in the structures, and so for the sake of brevity we provide a generic description of the metallic $[\mathrm{Co^{II}}_6\mathrm{Ln^{III}}]$ species. Selected bond distances and bond angles are provided in Tables S3−S13 of the Supporting Information. Their metallic core consists of a $\mathrm{Co^{II}}_6$ trigonal prism which encapsulates one $\mathrm{Ln^{III}}$ *via* six $\eta^2{:}\eta^1{:}\eta^1{:}\mu_3$ deprotonated $\mathrm{aib^-}$ ligands, with each one bridging two $\mathrm{Co^{II}}$ ions and the $\mathrm{Ln^{III}}$ center, and three μ_3-$\mathrm{OH^-}$ ligands. Furthermore, for all **4**−**11** and **13** complexes, there are three μ-$\mathrm{NO_3^-}$ ligands acting as a monatomic bridge, with each one bridging two $\mathrm{Co^{II}}$ ions via one $\mathrm{O_{NO_3}}^-$ atom, while for **2** only two μ-$\mathrm{NO_3^-}$ ligands are present. In addition, for **12** one μ-$\mathrm{NO_3^-}$ ligand is "replaced" by a μ-$\mathrm{OH^-}$ ligand. The $\mathrm{Ln^{III}}$ ion is located within a cage formed by three macrocycles assembled in a trigonal prismlike fashion, with the threading points being adjacent $\mathrm{Co^{II}}$ centers (Figure 3, right). All $\mathrm{Co^{II}}$ ions are six-coordinate,

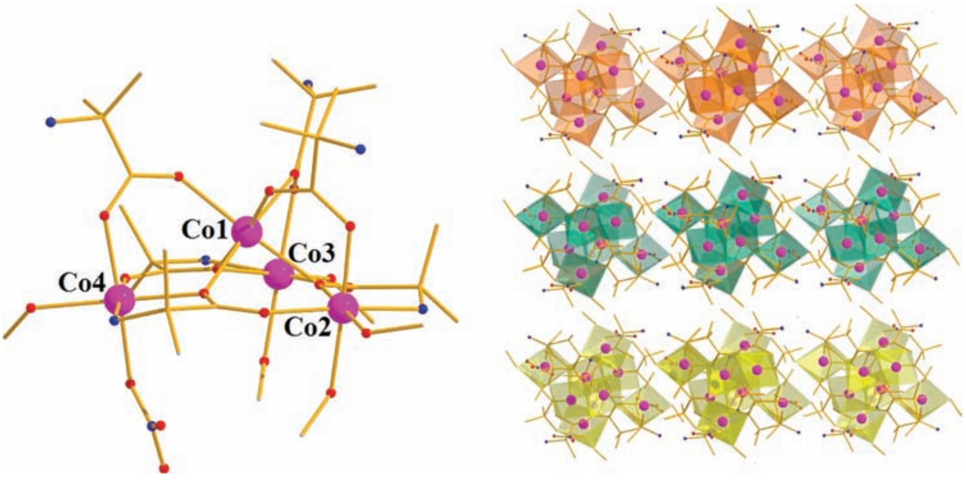

Figure 1. Molecular structure of the cation of complex **1** (left). The crystal packing of the cations in **1** (right). The differently colored $\mathrm{Co^{II}}$ polyhedra indicate molecules belonging to neighboring sheets. Color code: Co(II) = pink; O = red; N = blue; C = gold.

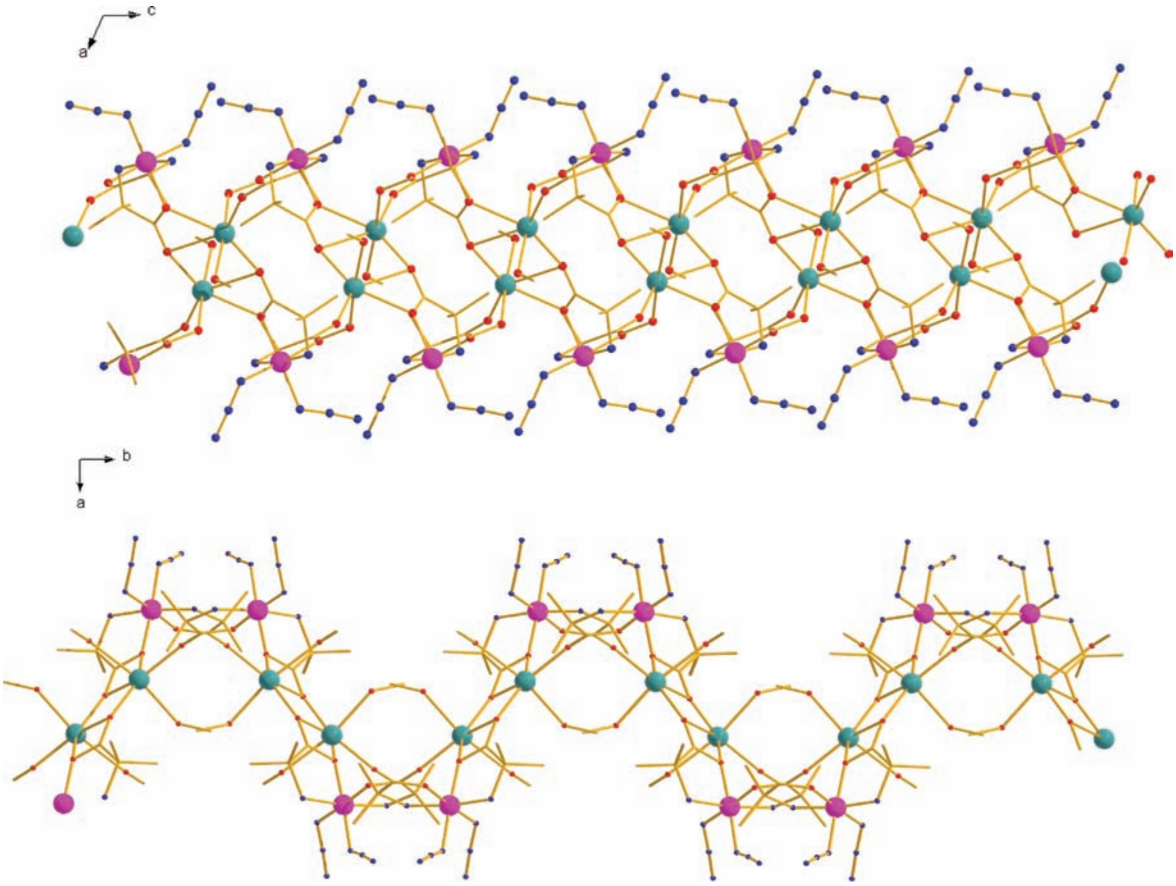

Figure 2. Two perspective views of the crystal structure of **2** as viewed on the *ac* (top) and *ab* (bottom) plane. Color code: Co^{II} = pink; Na^{+} = green; O = red; N = blue; C = yellow.

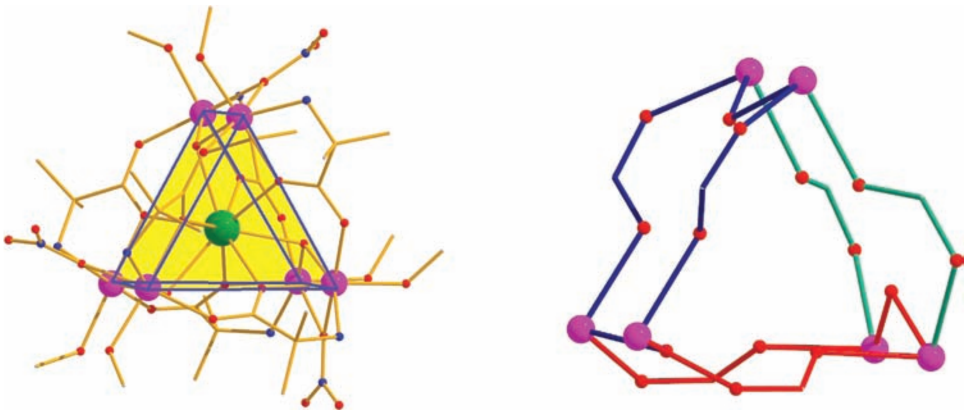

Figure 3. Molecular structure of the $[Co_6Ln]$ complexes **3**−**13**, highlighting the trigonal prismatic conformation (left); the cagelike formation in **3**−**13** responsible for the entrapment of the Ln^{III} center. Color code: Co(II) = pink; Ln(III) = green; O = red; N = blue; C = gold.

adopting distorted octahedral geometries with $[O_5N]$ coordination spheres, while the central Ln^{III} ion is nine-coordinate with an $[O_9]$ coordination sphere, adopting a tricapped trigonal prismatic geometry. The two $[Co_3{}^{II}]$ triangles forming the trigonal prism are almost equilateral (Co···Co ∼ 5.4 Å), while the depth of the trigonal prism is ∼3.4 Å and capable of fully encapsulating the Ln^{III} ions (the Ln^{III} radii are in the 1.02−0.86 Å range, Ce^{III}−Lu^{III}). The Co^{II}−Ln^{III} distance is ∼3.5 Å, while the Ln^{III} center is located at the center of the trigonal prism at 1.7 Å from the two $[Co_3{}^{II}]$ triangles. Alternatively, the metallic core may be described as a $[Co_6Ln(OR)_6(OH)_3]^{6+}$ propeller-like structure in which the central Ln^{III} ion is connected to three $[Co^{II}{}_2(OR)_2(OH)]$ species (Figure 4).

As in the case of **1**, the highly disordered counterions and/or solvate molecules present in complexes **3**−**13** do not allow us to draw safe conclusions regarding the crystal packing/interactions of the complexes.

Previously reported $[Co_6Ln]$ clusters are restricted to two examples: (i) one cluster having the $[Co^{II}{}_5Co^{III}La]$ core made with use of the natural occurring amino acid proline, in which the central La^{III} ion is located at the center of a Co_6

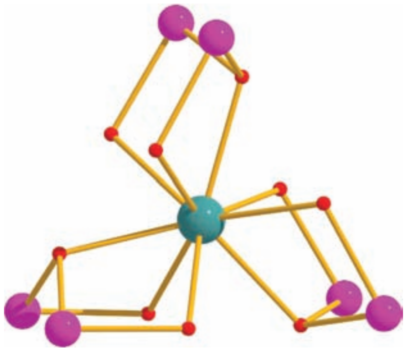

Figure 4. Propeller-like metallic core of **3**−**13**. Color code: same as in Figure 3.

octahedron[12a] and (ii) one $[Co^{II}_6Pr]$ cluster prepared with the use of glycine, adopting an octahedron captivated Pr^{III} ion.[12b] Finally, one other "Co_6Ln" compound is the impressive organometallic oxo-molybdenum cluster $[H_4Ce(Co(\eta^5\text{-Cp})\{P(O)(OEt)_2\}_3)_6Mo_9O_{38}]$.[12c]

dc Magnetic Susceptibility Studies. Variable temperature dc magnetic susceptibility data were collected for all complexes **1**, **3**, **5**, **7**, **8**, **10**, **12**, and **13** in the temperature range 5.0−300 K under an applied field of 0.1 T. These are plotted as $\chi_M T$ versus T in Figure 5.

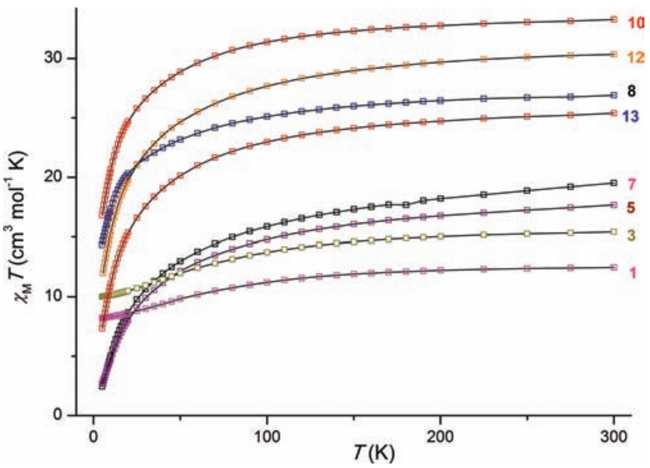

Figure 5. Plot of $\chi_M T$ *vs* T for complexes **1**, **3**, **5**, **7**, **8**, **10**, **12**, and **13** under an applied dc field of 1000 G. The straight lines are guides for the eye only.

For **1**, the room temperature $\chi_M T$ value of 12.17 cm^3 K mol^{-1} corresponds to four noninteracting Co^{II} ions with $S = {}^3/_2$ and $g = 2.55$. Upon cooling, the $\chi_M T$ value remains almost constant until ~100 K, below which it decreases to a minimum value of 8.86 cm^3 K mol^{-1} at 5 K. Given the presence of octahedral Co^{II} ions with a $^4T_{1g}$ ground term, as verified by means of solid-state UV−vis spectroscopy (*vide infra*), that splits to a doublet ground state at low temperature when in a distorted environment due to spin−orbit coupling,[16] it is very laborious and extremely difficult to apply an exact theoretical model for fitting the magnetic susceptibility data.[17] For example, one could attribute the low temperature value to an $S = 3$ ground state assuming $g = 2.55$. However, such a conclusion should be considered with great caution since Co(II) is highly anisotropic and the magnetic exchange interactions in such systems are mainly dictated by the orientation of the local magnetic moments.[18] In addition, one should remember that Co(II) ions in octahedral symmetry may be treated as pseudo "$s_{eff} = {}^1/_2$" systems at low temperature due to the splitting of the Kramers doublets. Nevertheless, evidence supporting the presence of dominant antiferromagnetic interactions comes from a Curie−Weiss analysis of the high temperature (50−300 K) magnetic susceptibility data with $\theta = -17$ K (Figure 6, left) and from the M *vs* H data (Figure 6, right), where M increases only slowly with the applied magnetic field, as one would expect from an antiferromagnetic compound, rather than saturating quickly, as one might expect from a ferromagnetic compound.

For the $[Co_6Ln]$ clusters the situation is far more complicated, since, besides the Co^{II} ions, anisotropic lanthanides also contribute to the magnetic moments and play a major role in the magnetic behavior of the complexes. Each Ln^{III} center is susceptible to interelectronic repulsions and spin−orbit coupling effects that lead to $^{2S+1}L_J$ states, which are further split due to crystal field perturbation to the Stark sublevels for each $^{2S+1}L_J$ state. The simplest case is complex **3**, which hosts a diamagnetic lanthanide (La^{III}). For **3**, the room temperature $\chi_M T$ value of 15.49 cm^3 K mol^{-1} corresponds to six noninteracting Co^{II} ions with $S = {}^3/_2$ and $g = 2.34$. Upon cooling, the $\chi_M T$ value gradually decreases to a minimum value of 9.99 cm^3 K mol^{-1} at 5 K, with the low temperature value suggesting an $S \approx 3$ ground state (for $g = 2.34$). For **5** and **7**, the same behavior is observed; the room temperature $\chi_M T$ values of 16.97 and 18.14 cm^3 K mol^{-1} are very close to the theoretical values for six noninteracting Co^{II} ions with $S = {}^3/_2$ and $g = 2.34$ and (i) one Nd^{III} ($^4I_{9/2}$, $S = {}^3/_2$, $L = 6$, $J = {}^9/_2$, $g_j = 0.74$) for **5** of 17.18 cm^3 K mol^{-1} and (ii) one Eu^{III} ($^7F_0$, $S = 3$, $L = 3$, $J = 0$) of 18.10 cm^3 K mol^{-1} for **7**. For the latter, although in principle the europium center should not contribute to the magnetic moment of the complex, since its ground term is $^7F_0$ with $J = 0$, usually some contribution from thermally accessible levels such as $^7F_1$ and $^7F_2$ appears.[6] For **8** and **10** the room temperature $\chi_M T$ values of 26.19 and 33.35 cm^3 K mol^{-1} are very close to the theoretical values for six noninteracting Co^{II} ions with $S = {}^3/_2$ and $g = 2.53$ and (i) one Gd^{III} ($^8S_{7/2}$, $S = {}^7/_2$, $L = 0$, $J = {}^7/_2$, $g_j = 2.00$) for **8** of 25.88 cm^3 K mol^{-1} and (ii) one Dy^{III} ($^6H_{15/2}$, $S = 5/2$, $L = 5$, $J = 15/2$, $g_j = 1.33$) for **10** of 32.26 cm^3 K mol^{-1}, respectively. Finally, for **12** and **13** the room temperature $\chi_M T$ values of 30.30 and 25.33 cm^3 K mol^{-1} are very close to the theoretical values for six noninteracting Co^{II} ions with $S = {}^3/_2$ and $g = 2.53$ and (i) one Er^{III} ($^4I_{15/2}$, $S = {}^3/_2$, $L = 6$, $J = {}^{15}/_2$, $g_j = 1.20$) for **12** of 29.50 cm^3 K mol^{-1} and (ii) one Tm^{III} ($^3H_6$, $S = 2$, $L = 5$, $J = 6$, $g_j = 1.17$) for **13** of 25.16 cm^3 K mol^{-1}. For complexes **5** and **7**, upon cooling, the $\chi_M T$ value gradually decreases to a minimum value of ~2.5 cm^3 K mol^{-1} at 5 K, indicating the presence of dominant antiferromagnetic interactions and/or the depopulation of the lanthanide Stark sublevels. For complex **8**, the decrease of the $\chi_M T$ value upon cooling should be attributed mainly to antiferromagnetic interactions within the cluster, since for Gd^{III} there is a unique Stark component.[19] For complexes **8**, **10**, and **12**, despite the fact that upon cooling the $\chi_M T$ value gradually decreases, the low temperature $\chi_M T$ values at 5 K of 16.51 and 12.01 cm^3 K mol^{-1}, respectively, indicate the presence of significant remaining magnetic moment.

In general, for all $[Co^{II}_6Ln^{III}]$ complexes studied, the decrease of the $\chi_M T$ values upon cooling should

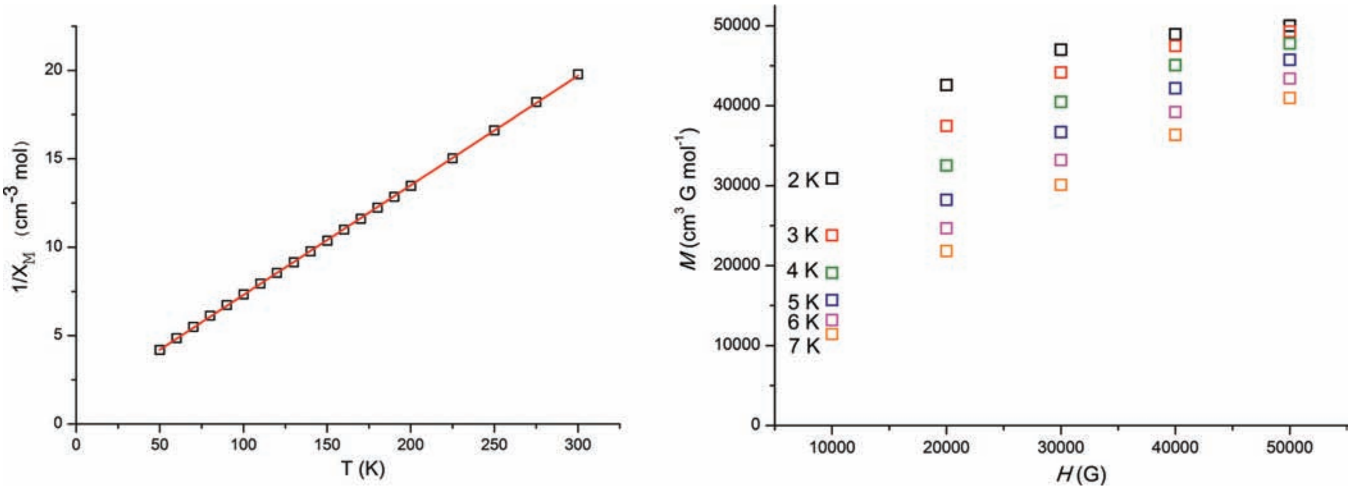

Figure 6. Curie−Weiss plot for complex **1** for the 50−300 K range (left); *M* vs *H* isotherms for complex **1** in the 2−5 K and 1−5 T range (right).

be attributed to the depopulation of the Stark sublevels of the Ln^{III} centers, and/or the presence of spin−orbit coupling for octahedral Co^{II} ions, and/or the intramolecular antiferromagnetic interactions between the metal centers.[20]

ac Magnetic Susceptibility Studies. ac magnetic susceptibility measurements were performed on polycrystalline samples of complexes **1**, **8**, **9**, **10**, **12**, and **13** in the 1.8−10 K range in zero applied dc field and 1.0 G ac field oscillating in the 100−1000 Hz range. For all samples measured, the in-phase (χM′, plotted as χM′T vs *T*, Figure 7) signal decreases upon decreasing temperature, indicating either the presence of low-lying excited states with larger "*S*" values than those of the ground-state and/or the depopulation of the lanthanide Stark sublevels with decreasing temperature, in agreement with the dc measurements. For complex [Co$_6$Dy] **10** frequency-dependent out-of-phase (χ_M'') signals are observed below ~3 K, but no peaks are seen (Figure 8), indicating the possibility of single molecule magnetism behavior, albeit with a small barrier to magnetization reversal.

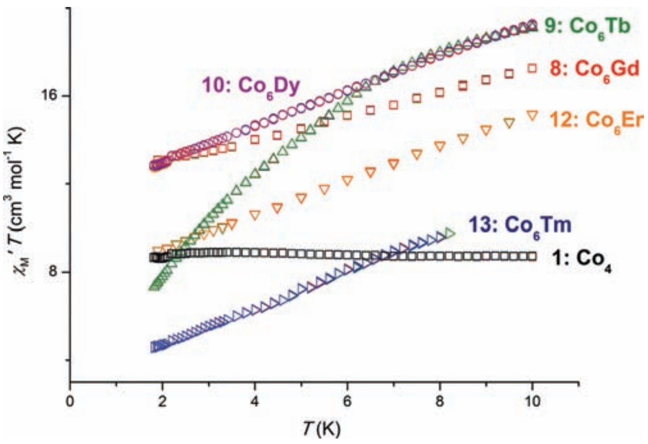

Figure 7. Plot of the in-phase (χ_M′) signal as χ_M′*T* vs temperature for complexes **1**, **8**, **9**, **10**, **12**, and **13** in a 1.0 G field oscillating in the 100−1000 Hz frequency range.

Absorption Spectroscopy. The solid-state electronic absorption spectra of complexes **5**, **7**, **9**, and **10** are shown in Figure 9. All complexes display a similar pattern in the 200−600 nm region, with the high energy absorption at ~270 nm corresponding to the Ln^{III} f−d transition, while the peaks at ~455 and 535 nm, as well as the shoulder at ~630 nm, may be attributed to octahedral Co^{II} ions and more specifically to the $^4T_{1g} \rightarrow {}^4T_{1g}$ (P) and $^4T_{1g} \rightarrow {}^4A_{2g}$ transitions, respectively.[21] This complicated structure is due to spin−orbit coupling effects and admixture of spin forbidden transitions to doublet states. Furthermore, complex **6** displays two further bands at ~742 and ~805 nm whose line shapes are diagnostic and informative for the existence of a nine-coordinate Nd(III) ion. These bands are due to the $^4I_{9/2} \rightarrow {}^4F_{7/2}$, $^4S_{3/2}$ and $^4I_{9/2} \rightarrow {}^2H_{9/2}$, $^4F_{5/2}$ transitions, respectively.[22] Finally, the band at ~876 nm may be attributed to the $^4I_{9/2} \rightarrow {}^4F_{3/2}$ transition.

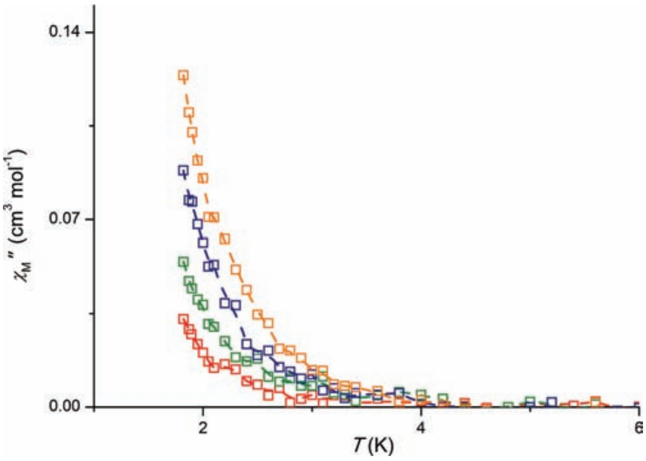

Figure 8. Plot of the out-of-phase (χ_M″) signal vs temperature for **10** in a 1.0 G field oscillating at 100 (red squares), 200 (green squares), 500 (blue squares), and 1000 (orange squares) Hz frequency.

The complexes retain their solid-state UV−vis spectroscopic features almost intact in MeCN solution (Figure 9, inset), suggesting that the structure is maintained when the complexes are dissolved in MeCN, as was evidenced by means of ES-MS spectroscopy.[10]

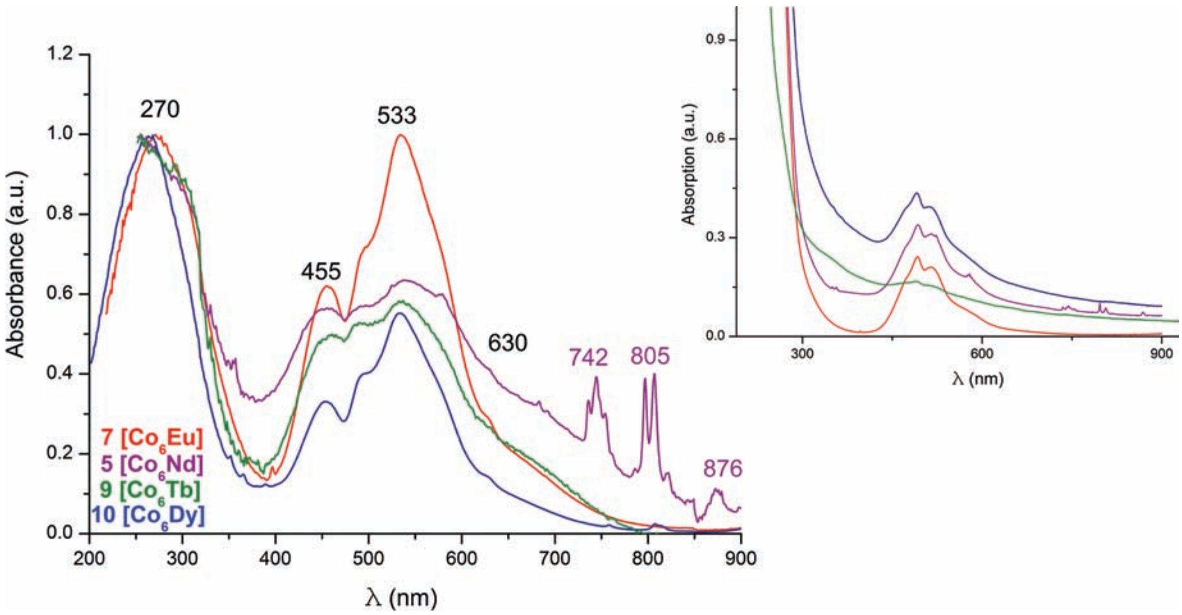

Figure 9. Solid-state and solution (inset) UV−vis spectra for complexes **5**, **7**, **9**, and **10**.

■ CONCLUSIONS

The use of the artificial amino acid 2-aminoisobutyric acid, aibH, in $\mathrm{Co^{II}}$ and $\mathrm{Co^{II}}/\mathrm{Ln^{III}}$ chemistry has led to the synthesis of 14 new homo- and heterometallic complexes. These synthetic systems are sensitive to the presence of base that dictates the formation of either lanthanide-free $\mathrm{Co^{II}}$ clusters or heterometallic $\mathrm{Co^{II}}/\mathrm{Ln^{III}}$ complexes. The magnetic properties of all complexes studied followed the same "trend". More specifically, for the 12 $[\mathrm{Co^{II}}_6\mathrm{Ln^{III}}]$ derivatives studied magnetically, from $\mathrm{La^{III}}$ to $\mathrm{Tm^{III}}$, all complexes display similar behavior with decreasing $\chi_M T$ values upon cooling, leading to small ground states, with the only exception being the Dy analogue (**10**), which displays out-of-phase signals suggesting the possibility of single molecule magnetism behavior, albeit with a small barrier to magnetization reversal, U_{eff}.

■ ASSOCIATED CONTENT

Ⓢ Supporting Information

Tables of selected bond distances and angles for **1**−**13**, and crystallographic data in CIF format. This material is available free of charge via the Internet at http://pubs.acs.org.

■ AUTHOR INFORMATION

Corresponding Author

*E-mail: komil@chemistry.uoc.gr.

■ ACKNOWLEDGMENTS

C.J.M. thanks The University of Crete (ELKE, research grant KA 3089) for funding. C.J.M. would also like to thank D. Anglos (Department of Chemistry, UoC) for fruitful discussions.

■ REFERENCES

(1) Representative references and references therein: (a) Que, E. L.; Chang, C. J. *Chem. Soc. Rev.* **2010**, *39*, 51. (b) Fricker, S. P. *Chem. Soc. Rev.* **2006**, *6*, 524. (c) Murray, L. J.; Dincă, M.; Long, J. R. *Chem. Soc. Rev.* **2009**, *38*, 1294. (d) Manoli, M.; Collins, A.; Parsons, S.; Candini, A.; Evangelisti, M.; Brechin, E. K. *J. Am. Chem. Soc.* **2008**, *130*, 11129. (e) Bogani, L.; Wernsdorfer, W. *Nat. Mater.* **2008**, *7*, 179.

(2) (a) Gatteschi, D.; Sessoli, R. *Angew. Chem., Int. Ed.* **2003**, *42*, 268. (b) Christou, G.; Gatteschi, D.; Hendrickson, D. N.; Sessoli, R. *MRS Bull.* **2000**, *25*, 66.

(3) For reviews, see: (a) Aromi, G.; Brechin, E. K. *Struct. Bonding (Berlin)* **2006**, *122*, 1. (b) Christou, G.; Gatteschi, D.; Hendrickson, D. N.; Sessoli, R. *MRS Bull.* **2000**, *25*, 66. (c) Gatteschi, D.; Sessoli, R. *Angew. Chem., Int. Ed.* **2003**, *42*, 268. (d) Bircher, R.; Chaboussant, G.; Dobe, C.; Güdel, H. U.; Ochsenbein, S. T.; Sieber, A.; Waldman, O. *Adv. Funct. Mater.* **2006**, *16*, 209.

(4) (a) Sessoli, R.; Powell, A. K. *Coord. Chem. Rev.* **2009**, *253*, 2328. (b) Papatriantafyllopoulou, C.; Stamatatos, T.; Efthymiou, C. G.; Cunha-Silva, L.; Paz, F. A. A.; Perlepes, S. P.; Christou, G. *Inorg. Chem.* **2010**, *49*, 9743. (c) Efthymiou, C. G.; Stamatatos, T. C.; Papatriantafyllopoulou, C.; Tasiopoulos, A. J.; Wernsdorfer, W.; Perlepes, S. P.; Christou, G. *Inorg. Chem.* **2010**, *49*, 9739. (d) Mishra, A.; Wernsdorfer, W.; Parsons, S.; Christou, G.; Brechin, E. K. *Chem. Commun.* **2005**, 2086. (e) Mereacre, V.; Ako, A. M.; Clèrac, R.; Wernsdorfer, W.; Hewitt, I. J.; Anson, C. E.; Powell, A. K. *Chem.—Eur. J.* **2008**, *14*, 3577. (f) Abbas, G.; Lan, Y.; Mereacre, V.; Wernsdorfer, W.; Clèrac, R.; Buth, G.; Sougrati, M. T.; Grandjean, F.; Long, G. J.; Anson, C. E.; Powell, A. K. *Inorg. Chem.* **2009**, *48*, 9345. (g) Baskar, V.; Gopal, K.; Helliwell, M.; Tuna, F.; Wernsdorfer, W.; Winpenny, R. E. P. *Dalton Trans.* **2010**, *39*, 4747. (h) Chandrasekhar, V.; Pandian, B. M.; Boomishankar, R.; Steiner, A.; Vittal, J. J.; Houri, A.; Clèrac, R. *Inorg. Chem.* **2008**, *47*, 4918. (i) Rigaux, G.; Inglis, R.; Morrison, S.; Prescimone, A.; Cadiou, C.; Evangelisti, M.; Brechin, E. K. *Dalton Trans.* (DOI: 10.1039/c1dt10154d).

(5) Bünzli, J.-C. G.; Piguet, C. *Chem. Soc. Rev.* **2005**, *34*, 1048.

(6) Cotton, S. *Lanthanide and Actinide Chemistry*; John Wiley & Sons: West Sussex, 2006.

(7) Kido, J.; Okamoto, Y. *Chem. Rev.* **2002**, *102*, 2357.

(8) Stouwdam, J. W.; Hebbink, G. A.; Huskens, J.; Van Veggel, F. C. J. M. *Chem. Mater.* **2003**, *15*, 4604.

(9) Peristeraki, T.; Samios, M.; Siczek, M.; Lis, T.; Milios, C. J. *Inorg. Chem.* **2011**, *50*, 5175.

(10) Orfanoudaki, M.; Tamiolakis, I.; Siczek, M.; Lis, T.; Armatas, G. S.; Pergantis, S. A.; Milios, C. J. *Dalton Trans.* **2011**, *40*, 4793.

(11) For reviews, see: (a) Escuer, A.; Aromi, G. *Eur. J. Inorg. Chem.* **2006**, 4721. (b) Ribas, J.; Escuer, A.; Monfort, M.; Vicente, R.; Cortés, R.; Lezama, L.; Rojo, T. *Coord. Chem. Rev.* **1999**, *195*, 1027.

(12) (a) Komiyama, T.; Igarashi, S.; Hoshino, Y.; Yukawa, Y. *Chem. Lett.* **2005**, *34*, 300. (b) Zhang, J.-J.; Hu, S.-M.; Xiang, S.-C.; Wang, L.-S.; Li, Y.-M.; Zhang, H.-S.; Wu, X.-T. *J. Mol. Struct.* **2005**, *748*, 129.

(c) Yi, X.; Sung, H. H. Y.; Williams, I. D.; Leung, W.-H. *Chem. Commun.* **2008**, 3269.

(13) Aparna, K.; Krishnamurthy, S. S.; Nethaji, M.; Balaram, P. *Polyhedron* **1994**, *13*, 2993.

(14) Zhang, J.-J.; Hu, S.-M.; Xiang, S.-C.; Sheng, T.; Wu, X.-T.; Li, Y.-M. *Inorg. Chem.* **2006**, *45*, 7173.

(15) Katsoulakou, E.; Papaefstathiou, G. S.; Konidaris, K. F.; Pairas, G.; Raptopoulou, C.; Cordopatis, P.; Manessi-Zoupa, E. *Polyhedron* **2009**, *28*, 3387.

(16) (a) Carlin, R. L. *Magnetochemistry*; Springer-Verlag: Berlin, 1986. (b) Kahn, O. *Molecular Magnetism*; Wiley-VCH: NewYork, 1993.

(17) Representative references and references therein: (a) Klöwer, F.; Lan, Y.; Nehrkorn, J.; Waldmann, O.; Anson, C. E.; Powell, A. K. *Chem.—Eur. J.* **2009**, *15*, 7413. (b) Yang, E. C.; Hendrickson, D. N.; Wernsdorfer, W.; Nakano, M.; Zakharov, L. N.; Sommer, R. D.; Rheingold, A. L.; Ledezma-Gairaud, M.; Christou, G. *J. Appl. Phys.* **2002**, *91*, 7382. (c) Zhang, Y.-Z.; Wernsdorfer, W.; Pan, F.; Wang, Z.-M.; Gao, S. *Chem. Commun.* **2006**, 3302. (d) Waldmann, O.; Ruben, M.; Ziener, U.; Müller, P.; Lehn, J. M. *Inorg. Chem.* **2006**, *45*, 6535. (e) Andres, H.; Clemente-Juan, J. M.; Aebersold, M.; Güdel, J. M.; Coronado, E.; Buettner, H.; Kearly, G.; Melero, J.; Burriel, R. *J. Am. Chem. Soc.* **1999**, *121*, 10028. (f) Palii, A. V.; Tsukerblat, B. S.; Coronado, E.; Clement-Juan, J. M.; Borras-Almenar, J. J. *Inorg. Chem.* **2003**, *42*, 2455. (g) Banci, L.; Bencini, A.; Benelli, C.; Gatteschi, D.; Zanchini, C. *Struct. Bonding (Berlin)* **1982**, *52*, 37. (h) Boča, R. *Struct. Bonding (Berlin)* **2006**, *117*, 1. (i) Moragues-Canovás, M.; Talbot-Eeckelaers, C. E.; Catala, L.; Lloret, F.; Wernsdorfer, W.; Brechin, E. K.; Mallah, T. *Inorg. Chem.* **2006**, *45*, 7038. (j) Clemente-Juan, J. M.; Coronado, E.; Gaita-Ariño, A.; Giménez-Saiz, C.; Güdel, H.-U.; Sieber, A.; Bircher, R.; Mutua, H. *Inorg. Chem.* **2005**, *44*, 3389. (k) Clemente-Juan, J. M.; Coronado, E.; Forment-Aliaga, A.; Galan-Mascaros, J. R.; Gimenez-Saiz, C.; Gomez-Garcia, C. J. *Inorg. Chem.* **2004**, *43*, 2689.

(18) Boeer, A. B.; Barra, A.-L.; Chibotaru, L. F.; Collison, D.; McInnes, E. J. L.; Mole, R. A.; Simeoni, G. G.; Timco, G. A.; Ungur, L.; Unruh, T.; Winpenny, R. E. P. *Angew. Chem., Int. Ed.* **2011**, *50*, 4007.

(19) (a) Couture, L. *J. Lumin.* **1979**, *18*, 891. (b) Kahn, M. L.; Mathonière, C.; Kahn, O. *Inorg. Chem.* **1999**, *38*, 3692.

(20) See for example: (a) Chandrasekhar, V.; Pandian, B. M.; Vittal, J. J.; Clérac, R. *Inorg. Chem.* **2009**, *48*, 1148 and references therein. (b) Chandrasekhar, V.; Pandian, B. M.; Azhakar, R.; Vittal, J. J.; Clérac, R. *Inorg. Chem.* **2007**, *46*, 5140.

(21) (a) Lever, A. B. P. *Inorganic Electronic Spectroscopy*, 2nd ed.; Elsevier: Amsterdam, 1984. (b) Galloway, K. W.; Whyte, A. M.; Wernsdorfer, W.; Sanchez-Benitez, J.; Kamenev, K. V.; Parkin, A.; Peacock, R. D.; Murrie, M. *Inorg. Chem.* **2008**, *47*, 7438. (c) Tiliakos, M.; Cordopatis, P.; Terzis, A.; Perlepes, S. P.; Manessi-Zoupa, E. *Polyhedron* **2001**, *20*, 2203. (d) Plakatouras, J. C.; Perlepes, S. P.; Mentzafos, D.; Terzis, A.; Bakas, T.; Papaefthymiou, V. *Polyhedron* **1992**, *11*, 2657. (e) Vakros, J.; Bourikas, K.; Perlepes, S.; Kordulis, C.; Lycourghiotis, A *Langmuir* **2004**, *20*, 10542.

(22) (a) Sastri, V. S.; Bünzli, J.-C. G.; Rao, V. R.; Rayudu, G. S. V.; Perumareddi, J. R. *Modern Aspects Of Rare Earths And Their Complexes*; Elsevier: Amsterdam, 2003. (b) Karraker, D. G. *Inorg. Chem.* **1968**, *7*, 473.